Implications of different classes of sensorimotor disturbance for cerebellar-based motor learning models

Biological Cybernetics manuscript No.
(will be inserted by the editor)

Adrian Haith · Sethu Vijayakumar

Implications of different classes of sensorimotor disturbance for cerebellar-based motor learning models

Received: date / Revised: date

Abstract The exact role of the cerebellum in motor control and learning is not yet fully understood. The structure, connectivity and plasticity *within* cerebellar cortex has been extensively studied, but the patterns of connectivity and interaction with other brain structures, and the computational significance of these patterns, is less well known and a matter of debate.

Two contrasting models of the role of the cerebellum in motor adaptation have previously been proposed. Most commonly, the cerebellum is employed in a purely feedforward pathway, with its output contributing directly to the outgoing motor command. The cerebellum must then learn an inverse model of the motor apparatus in order to achieve accurate control. More recently, Porrill *et al.* (2004) have advocated the possibility of a recurrent architecture, in which the cerebellum is embedded in a recurrent loop with brainstem control circuitry. In this framework, the cerebellum must learn a forward model of the motor apparatus for accurate motor commands to be generated. We show here how these two models exhibit contrasting yet complimentary learning capabilities.

Central to the differences in performance between architectures is that there are two distinct kinds of disturbance to which a motor system may need to adapt i) changes in the relationship between the motor command and the observed outcome and ii) changes in the relationship between the stimulus and the desired outcome. The computational distinction between these two kinds of transformation is subtle and has therefore often been overlooked. However, the implications for learning turn out to be significant: learning with a feedforward architecture is robust following changes in the stimulus-desired outcome mapping but not necessarily the motor command-outcome mapping, while learning with a recurrent architecture is robust under changes in the motor command-outcome mapping but not necessarily the stimulus-desired outcome mapping. We analyse these differences theoretically and through simulations in the context of three extensively-studied motor behaviours: the vestibulo-ocular reflex (VOR), saccades and reaching.

Adrian Haith · Sethu Vijayakumar
Institute of Perception, Action and Behaviour
University of Edinburgh, Edinburgh EH9 3JZ, UK
E-mail: adrian.haith@ed.ac.uk

1 Introduction

Humans and non-human primates demonstrate a remarkable ability to adapt their motor behaviour to novel circumstances and to learn to perform new motor tasks. The need to adapt existing controllers may arise for a variety of reasons including growth, ageing, injury, disease or experimental intervention in the laboratory. Acquisition of accurate motor behaviour from birth during infancy also requires similar or perhaps even identical learning mechanisms to motor learning during adulthood.

In general, a motor control task involves generating appropriate motor commands in response to some stimulus to bring about a desired outcome. There are two fundamental types of change which can alter what the appropriate motor commands are in response to a given stimulus (see Fig. 1). Firstly, the relationship between the motor commands and the resulting outcome can be altered. This typically involves changes in the motor plant dynamics (e.g. through injury, disease, growth or ageing); however some changes which are more kinematic in nature, such as distortions of visual feedback, can also be grouped into this category.

A second kind of change is in the relationship between the initial stimulus and the desired outcome following that stimulus. This kind of change is more subtle than the previous one but examples do occur in the context of most motor behaviours - either naturally or under experimental conditions. After such a change, the original response to the stimulus will no longer be appropriate and a new pattern of responses must be learnt.

In many circumstances, the stimulus and the desired outcome can be considered to be equivalent. For exam-

ple, in the case of reaching, the stimulus is the location of an object in the visual field and the desired outcome is that the hand be in that same location (note that this is true even when visual feedback is tampered with). Nevertheless, there are numerous examples where the stimulus-desired outcome relationship is not so trivial and subject to change. As we will describe in later sections, many common experimental paradigms in oculomotor adaptation actually fall into the latter category rather than the former. Adaptation to these kinds of changes can also be induced in reaching tasks (Lurito *et al.* 1991) where they are sometimes referred to as 'non-standard mappings' or 'transformational mappings' (Shadmehr and Wise 2005).

The possibility of having to adapt in the face of an unknown relationship between the stimulus and the desired outcome has been noted before (Jordan and Rumelhart 1992), but a thorough examination of the extent to which this applies to human motor system in practice has been previously lacking: Indeed, the solutions proposed in (Jordan and Rumelhart 1992) do not aim at biological plausibility since they rely on backpropagation of error signals through a learnt internal model.

We examine the problem of adapting to both kinds of change from a biologically plausible cerebellar learning perspective. In the next section, we describe in detail two existing models of cerebellar-based motor learning in the context of a variety of commonly studied motor behaviours and examine their suitability for adapting to each of the two kinds of change described above.

Before going into the details of the different architectures, we will first illustrate the discussion with a concrete example in which both kinds of sensorimotor change occur naturally - the vestibulo-ocular reflex (VOR).

[Fig. 1 about here.]

1.1 Kinematics and Dynamics of the VOR

The vestibulo-ocular reflex in mammals acts to stabilize gaze during head rotations by counter-rotating the eyes. The characteristics of this reflex are not fixed, but can be modified through experience when conditions change. After a suitable amount of training under these new conditions, the VOR becomes recalibrated so that even in the dark, the response of the VOR is altered (Lisberger *et al.* 1994).

[Fig. 2 about here.]

Denoting the current eye position by $\mathbf{y}$, the relationship between the motor command $\mathbf{u}$ and the resulting eye velocity $\dot{\mathbf{y}}$ (see Fig. 2) is determined by the forward dynamics of the oculomotor plant,

$$\dot{\mathbf{y}} = P(\mathbf{y}, \mathbf{u}). \tag{1}$$

The inverse dynamics model is correspondingly defined as

$$\mathbf{u} = P^{-1}(\mathbf{y}, \dot{\mathbf{y}}). \tag{2}$$

The inverse dynamics P^{-1} map the current eye position $\mathbf{y}$ and eye velocity $\dot{\mathbf{y}}$ to a motor command $\mathbf{u}$ which would achieve that eye velocity when acting through the plant.

The desired outcome in this case is that the gaze be stabilized, i.e. that the eye velocity $\dot{\mathbf{y}}$ be equal to some gaze-stabilizing eye velocity $\dot{\mathbf{y}}^*$. Any deviations of eye velocity from this desired value will be perceived as retinal slip - movement of the visual image across the retina. We denote this retinal slip by $\dot{\tilde{\mathbf{y}}}$ and it is given by

$$\dot{\tilde{\mathbf{y}}} = \dot{\mathbf{y}}^* - \dot{\mathbf{y}}. \tag{3}$$

We define $\mathbf{u}^*$ as the motor command which achieves the desired eye velocity $\dot{\mathbf{y}}^*$ when supplied to the plant,

$$\mathbf{u}^* = P^{-1}(\mathbf{y}, \dot{\mathbf{y}}^*). \tag{4}$$

In most VOR models, desired eye velocity is taken as equal and opposite to head velocity, i.e. $\dot{\mathbf{y}}^* = -\dot{\mathbf{x}}$. However, in general, this is not the case.

Most VOR gain adaptation experiments work by directly manipulating the relationship between head velocity and desired eye velocity, not by changing the properties of the oculomotor plant. This includes any experiment using prisms or lenses or vestibular mismatch experiments in which an external visual stimulus is moved in phase with head movements.

VOR adaptation therefore cannot be regarded as simply a process of learning the motor command-outcome mapping of the oculomotor plant. Fundamental to VOR adaptation is that the relationship between the stimulus (head velocity) and the desired outcome (gaze-stabilizing eye velocity) is also subject to change and must be compensated for, as illustrated in Fig. 2.

Mathematically, we can describe this relationship as a function mapping head velocity $\dot{\mathbf{x}}$ and current eye position $\mathbf{y}$ to a desired eye velocity $\dot{\mathbf{y}}^*$,

$$\dot{\mathbf{y}}^* = S(\mathbf{y}, \dot{\mathbf{x}}) \tag{5}$$

and a corresponding inverse kinematics mapping

$$\dot{\mathbf{x}}' = S^{-1}(\mathbf{y}, \dot{\mathbf{y}}). \tag{6}$$

S maps the current head velocity $\dot{\mathbf{x}}$ to an appropriate gaze-stabilizing eye velocity $\dot{\mathbf{y}}$, while S^{-1} gives the head rotation $\dot{\mathbf{x}}'$ that would have required an eye movement $\dot{\mathbf{y}}$ to stabilize gaze.

In general, the kinematic mapping S incorporates effects due to distortion of the visual image before reaching the eye, movements of the external scene which are correlated with head movement (visual-vestibular mismatch), off-axis effects (Coenen and Sejnowski 1996) and inaccuracies or nonlinearities in the vestibular measurements of $\dot{\mathbf{x}}$. VOR adaptation must, either explicitly or implicitly,

reflect learning of this kinematic relationship as well as of the plant dynamics.

Hence, from (2) and (5), the overall mapping which must be learnt is a composite function

$$\mathbf{u}^* = P^{-1}(\mathbf{y}, S(\mathbf{y}, \dot{\mathbf{x}})). \tag{7}$$

This shows exactly how each kind of mapping, stimulus-desired outcome or motor command-outcome, influences the choice of motor command $\mathbf{u}$.

In later sections, we will give further examples of behaviours where both of these kinds of mappings are subject to change. First, however, we show the implications that changes in each of these kinds of mappings has for different models of cerebellar-based adaptation.

2 Cerebellar-based learning models

We now analyse in more detail the alternative architectures for cerebellar connectivity with other brain regions and the implications for learning. In this section, we describe a model of cerebellar-based VOR adaptation. The VOR is used here as an illustrative example, particularly because the underlying neuroanatomy has been extensively studied. The arguments we make in this section, however, are quite general and central to the theme of this paper.

It is well known that the cerebellum plays a crucial role in VOR adaptation. The VOR is known to be mediated by a fast three-synapse pathway in the brainstem. This brainstem pathway is augmented by an adaptive pathway through the cerebellum. It is known that among its many inputs, the region of the cerebellum involved in the VOR receives the same vestibular input as the brainstem, and also an efferent copy of the outgoing motor command (Hirata and Highstein 2001). Most VOR models have tended to disregard these efferent copies, modelling the brainstem and cerebellar pathways as having a purely feedforward architecture (Gomi and Kawato 1990; Kawato and Gomi 1992; Shibata and Schaal 2001). This kind of feedforward organization is illustrated in Fig. 3(a). More recently, Porrill *et al.* (2004) have advocated a model of VOR adaptation with a recurrent cerebellar architecture, emphasizing the efferent motor command inputs, illustrated in Fig. 3(b).

Although the neuroanatomy underlying the VOR has been well-characterized, the computational significance of the different connections is not fully understood and is under debate. These two models represent different interpretations of the underlying anatomy. As we shall see, the choice of architecture (feedforward or recurrent) turns out to have a significant impact upon the learning properties of the model.

Before analysing the different architectures in detail, we briefly discuss a basic model of learning within cerebellar cortex.

2.1 Cerebellar Plasticity Model

For the purpose of illustration we will assume a simple Marr-Albus-Ito type model of cerebellar learning (Ito 2000). The arguments presented here, however, apply to any iterative error-driven learning scheme.

Let us denote the input to the cerebellum by $\mathbf{z}(t)$ and its output by $\mathbf{c}(t)$. In this model, the cerebellar output $\mathbf{c}(t) = C(\mathbf{z}(t))$ is given by a weighted sum of parallel fiber activities:

$$c_j(t) = \sum_i w_{ij} p_i(t),$$

where, $p_i(t)$ is the activity (i.e. firing rate) of the ith parallel fiber and w_i is the strength of the corresponding parallel fiber-Purkinje cell synapse. This can be written more compactly in vector notation as

$$\mathbf{c}(t) = \mathbf{w}^T \mathbf{p}(t). \tag{8}$$

Learning occurs through adaptation of the synaptic weights $\mathbf{w}$ over time. This is driven by the climbing fiber signal $\widetilde{\mathbf{c}}(t)$ which corresponds to the error in $\mathbf{c}(t)$ A simple learning rule which approximately captures the known plasticity laws at the synapses is

$$\dot{w}_{ij} = -\beta\, \widetilde{c}_j(t) p_i(t), \tag{9}$$

or in vector notation

$$\dot{\mathbf{w}} = -\beta\, \widetilde{\mathbf{c}}(t) \mathbf{p}(t)^T. \tag{10}$$

Although firing rates clearly cannot be negative, $\mathbf{p}(t)$ and $\widetilde{\mathbf{c}}(t)$ can be interpreted as deviations from some baseline firing rate. This learning rule is equivalent to performing gradient descent on the squared error, *provided* $\widetilde{\mathbf{c}}(t)$ *really does reflect the error in the cerebellar output.*

We do not, however, have explicit knowledge of the error in the cerebellar output. We can only measure the error in performance in terms of retinal slip. This poses a distal learning problem which can be solved by finding an appropriate mapping between the observed outcome error (retinal slip $\dot{\widetilde{\mathbf{y}}}$ in the case of the VOR) and the error in the cerebellar output $\widetilde{\mathbf{c}}$.

In order to calculate this, we need to know exactly what the desired output of the cerebellum is. This turns out to depend strongly on the architecture (feedforward or recurrent). Previous models of cerebellar VOR adaptation have only considered the effect of changes in the oculomotor plant dynamics (i.e. changes in the mapping between motor command and observed outcome). In this case (i.e. if we assume head velocity and desired eye velocity are equal and opposite), the error in the cerebellar output $\widetilde{\mathbf{c}}$ under the feedforward architecture is equal to the error in the motor command,

$$\widetilde{\mathbf{c}} = \mathbf{u}^* - \mathbf{u}. \tag{11}$$

This motor error can be estimated from the retinal slip by transforming it through an inverse model of the plant dynamics.

Under the recurrent architecture, on the other hand, Porrill *et al.* (2004) have shown that the error in the cerebellar output is equal to the raw retinal slip signal $\dot{\widetilde{\mathbf{y}}}$ and thus the distal learning problem is circumvented. However, both of these results were obtained by assuming that the desired eye velocity is exactly equal to the current head velocity which, as we have argued in the previous section, may not be the case.

We will now examine learning within each of these architectures in the case that the head velocity-eye movement relationship S is also subject to change. In both cases, we require an expression for the error in the cerebellar output, $\widetilde{\mathbf{c}}$, in terms of the observed output error (retinal slip, $\dot{\widetilde{\mathbf{y}}}$, in the case of the VOR).

[Fig. 3 about here.]

2.2 Learning in the Feedforward Architecture

Let us refer to the feedforward architecture shown in Fig. 3(a). The inputs to the cerebellum in this model are head velocity $\dot{\mathbf{x}}$ and head position $\mathbf{x}$ (omitted from the figure for clarity). We also assume that an optimal cerebellar model C^* exists (this corresponds to a set of optimal weights $\mathbf{w}^*$ for the cerebellum model outlined in the previous section). The error in the cerebellar output is then defined as

$$\widetilde{\mathbf{c}}(\mathbf{x}, \dot{\mathbf{x}}) = C^*(\mathbf{x}, \dot{\mathbf{x}}) - C(\mathbf{x}, \dot{\mathbf{x}}), \tag{12}$$

and we wish to express this in terms of the retinal slip $\dot{\widetilde{\mathbf{y}}}$.

The motor command is generated by combining the output from the brainstem and cerebellum

$$\mathbf{u} = C(\mathbf{x}, \dot{\mathbf{x}}) + B(\mathbf{x}, \dot{\mathbf{x}}), \tag{13}$$

where $B(\mathbf{x}, \dot{\mathbf{x}})$ describes the brainstem dynamics. Similarly for the optimal cerebellum model

$$\mathbf{u}^* = C^*(\mathbf{x}, \dot{\mathbf{x}}) + B(\mathbf{x}, \dot{\mathbf{x}}). \tag{14}$$

Noting that the optimal motor command $\mathbf{u}^*$ is given by $P^{-1}(\mathbf{y}, S(\mathbf{y}, \dot{\mathbf{x}}))$, we can see that the optimal cerebellum model C^* satisfies

$$C^*(\mathbf{x}, \dot{\mathbf{x}}) = P^{-1}(\mathbf{y}, S(\mathbf{y}, \dot{\mathbf{x}})) - B(\mathbf{x}, \dot{\mathbf{x}}). \tag{15}$$

The cerebellum must therefore learn a composite of a forward kinematics model and an inverse dynamics model, while compensating for the contribution from the brainstem B.

Now, taking the difference between (13) and (14) and comparing it to (12) illustrates that we can express the error in the cerebellar output as:

$$\widetilde{\mathbf{c}} = \mathbf{u}^* - \mathbf{u}, \tag{16}$$

that is, $\widetilde{\mathbf{c}}$ is equal to the *motor error*. Rewriting the right hand side of (16) in terms of the inverse plant model (2), we have

$$\widetilde{\mathbf{c}} = P^{-1}(\mathbf{y}, \dot{\mathbf{y}}^*) - P^{-1}(\mathbf{y}, \dot{\mathbf{y}}). \tag{17}$$

For linear plant dynamics, we can directly simplify and rewrite the expression in terms of the retinal slip $\dot{\widetilde{\mathbf{y}}}$,

$$\widetilde{\mathbf{c}} = P^{-1}(\mathbf{y}, \dot{\widetilde{\mathbf{y}}}). \tag{18}$$

For nonlinear plant dynamics, (17) can be approximated by the first term of the Taylor expansion of P^{-1} about $(\mathbf{y}, \dot{\mathbf{y}})$:

$$\widetilde{\mathbf{c}} \approx J_{P^{-1}}(\mathbf{y}, \dot{\mathbf{y}})\widetilde{\mathbf{y}}, \tag{19}$$

where $J_{P^{-1}}(\mathbf{y}, \dot{\mathbf{y}})$ is the Jacobian of P^{-1} at the point $(\mathbf{y}, \dot{\mathbf{y}})$.

Equations (18) and (19) show that the error in the cerebellar output can be calculated from the retinal slip via the inverse dynamics of the plant, i.e. the inverse of the mapping from motor commands to observed outcome. We assume that some internal model is available to compute this but if the plant dynamics change, an unadapted internal model will still reflect the old dynamics and we can no longer be confident that our estimate of the cerebellar output error is accurate.

The required training signal is, however, independent of the kinematics S, i.e. the relationship between the stimulus (head velocity $\dot{\mathbf{x}}$) and the desired outcome (eye velocity $\dot{\mathbf{y}}$). This is an important but usually overlooked advantage of employing a feedforward cerebellar architecture.

So, in general, we expect learning under the feedforward architecture to be impaired (i.e. converge more slowly) or even made entirely unstable (not converge at all) following a change in the motor command-outcome (dynamics) mapping. However, we expect learning to be unaffected by a change in the kinematics.

2.3 Learning in the Recurrent architecture

Next, we derive an expression for the error in the cerebellar output in terms of the measured retinal slip for the recurrent architecture (Fig. 3(b)). We assume that the inputs to the cerebellum are the head position $\mathbf{x}$ and the afferent motor command $\mathbf{u}$ (the head-position input is omitted in Fig. 3(b) for clarity).

We begin the derivation by noting that the input to the brainstem model is given by $C(\mathbf{x}, \mathbf{u}) + \dot{\mathbf{x}}$, which is equal to the motor command transformed under the brainstem inverse model, i.e.,

$$C(\mathbf{x}, \mathbf{u}) + \dot{\mathbf{x}} = B^{-1}(\mathbf{x}, \mathbf{u}). \tag{20}$$

Again, as in the feedforward case, we assume there exists an optimal cerebellar model C^* which yields exactly the

desired motor command (this corresponds to optimal weights $\mathbf{w}^*$ in the cerebellum model outlined previously).

Note that the motor command $\mathbf{u}$ would be optimal for some alternate head velocity $\dot{\mathbf{x}}'$, i.e.

$$C^*(\mathbf{x},\mathbf{u}) + \dot{\mathbf{x}}' = B^{-1}(\mathbf{x},\mathbf{u}), \tag{21}$$

with $\dot{\mathbf{x}}' = S^{-1}(\mathbf{y}, P(\mathbf{y},\mathbf{u}))$, by definition of S^{-1} from (1) & (6). Rearranging this, we have

$$C^*(\mathbf{x},\mathbf{u}) = B^{-1}(\mathbf{x},\mathbf{u}) - S^{-1}(\mathbf{y}, P(\mathbf{y},\dot{\mathbf{u}})). \tag{22}$$

Under the recurrent architecture then, the cerebellum must learn a composite of a forward dynamics model and an inverse kinematics model. This is in direct contrast to the feedforward case in (15).

Taking the difference between (20) and (21), we can express the cerebellar output error as:

$$\begin{aligned} C^*(\mathbf{x},\mathbf{u}) - C(\mathbf{x},\mathbf{u}) &= \dot{\mathbf{x}}' - \dot{\mathbf{x}} \\ &= S^{-1}(\mathbf{y},\dot{\mathbf{y}}) - S^{-1}(\mathbf{y},\dot{\mathbf{y}}^*). \end{aligned} \tag{23}$$

If we assume that S is linear then we can express this simply in terms of the retinal slip,

$$\widetilde{\mathbf{c}}(\mathbf{x},\mathbf{u}) = S^{-1}(\mathbf{y},\dot{\widetilde{\mathbf{y}}}). \tag{24}$$

If S is nonlinear, a first order Taylor approximation can be used,

$$\widetilde{\mathbf{c}} \approx J_{S^{-1}}(\mathbf{y},\dot{\mathbf{y}})\dot{\widetilde{\mathbf{y}}}, \tag{25}$$

where $J_{S^{-1}}(\mathbf{y},\dot{\mathbf{y}})$ is the Jacobian of S^{-1} at the point $(\mathbf{y},\dot{\mathbf{y}})$.

Equations (24) and (25) show that the error in the cerebellar output is given by the retinal slip transformed via the inverse kinematics, i.e. the inverse of the mapping from the stimulus to the desired outcome. This can be thought of as an error in the original vestibular signal $\dot{\mathbf{x}}$.

So in general, we expect learning under the recurrent architecture to be impaired under changes in the stimulus-desired outcome mapping, but to be unaffected by changes in the motor command-outcome mapping.

This reveals a duality between the feedforward and recurrent architecture models. The properties of learning in the feedforward architecture are mirrored by those of learning in the recurrent architecture with the roles of the two kinds of transformation transposed.

2.4 Summary

Although we have illustrated the argument with the specific example of the VOR, the arguments presented here are entirely general and can be applied to any other motor behaviour. Furthermore, the only point at which linearity was assumed was in the final step in each derivation combining the terms in Equations (17) and (23). For nonlinear P and S, a Taylor expansion gives a simple approximation to the cerebellar output error in terms of the observed output error, provided the error is not too large.

Under the feedforward architecture model, in order for the observed outcome error to act as an appropriate training signal for the cerebellum, it must be transformed into the motor domain via the motor command-outcome mapping. If this mapping changes drastically, for instance, through a change of the plant dynamics, the error signal being used may no longer accurately reflect the error in the cerebellar output and learning may proceed less efficiently or even be disrupted entirely. The transformed error is, however, independent of the head velocity-desired eye velocity mapping. Thus the feedforward architecture is guaranteed to learn stably following changes in this mapping.

For the recurrent architecture model, in order to train the cerebellum, the observed error must be transformed via the inverse of the stimulus-desired outcome mapping, giving something analogous to an error in the initial stimulus. If the true mapping from stimulus to desired outcome changes substantially, learning may be slowed down or even disrupted entirely. The transformation of the observed error into cerebellar output error is, however, independent of the motor command-outcome relationship and thus, the recurrent architecture is guaranteed to learn stably following a change in that mapping.

3 Simulation of VOR adaptation

[Fig. 4 about here.]

[Fig. 5 about here.]

In order to test the performance of each of the two alternative VOR models in adapting to a range of changes in both the motor command - outcome mapping and and the stimulus-desired outcome mapping, we simulated adaptation of a 2 degree-of-freedom oculomotor plant under a range of transformations of the kinematics and the plant dynamics. The simulated oculomotor plant had simplified dynamics initially given by

$$\dot{\mathbf{y}} = \mathbf{u}, \tag{26}$$

and an initial relationship between head velocity and gaze-stabilizing eye velocity given by

$$\dot{\mathbf{y}}^* = -\dot{\mathbf{x}}. \tag{27}$$

To simulate a change in the relationship between motor command and observed outcome, we changed the dynamics from the ordinary resistive viscosity field described by (26) to a viscous curl field (Fig. 4(a)) in which there is an angle ϕ between the eye velocity and the force, i.e.

$$\mathbf{u} = P_1\dot{\mathbf{y}}, \tag{28}$$

where

$$P_1 = \begin{pmatrix} \cos\phi & \sin\phi \\ -\sin\phi & \cos\phi \end{pmatrix}. \quad (29)$$

Due to the first-order dynamics assumed here, this had the effect of rotating the angle of actuation for a given motor command.

To change the relationship between head velocity and gaze-stabilizing eye velocity, we employed a rotation of the visual field (Fig. 4(b)) by angle ψ. Following this transformation, the desired eye velocity is rotated by angle ψ relative to the head velocity, i.e.

$$\dot{\mathbf{y}}^* = S_1 \dot{\mathbf{x}}^*, \quad (30)$$

where

$$S_1 = \begin{pmatrix} \cos\psi & \sin\psi \\ -\sin\psi & \cos\psi \end{pmatrix}. \quad (31)$$

In all experiments, the head position repeatedly traced out a figure-of-eight:

$$\mathbf{x}(t) = \begin{bmatrix} \sin(0.1t) \\ \sin(0.2t) \end{bmatrix}^T. \quad (32)$$

All experiments were run 10 times, with different initial positions around the figure-of-eight on each trial. Full implementation details are given in Appendix A.

3.1 Experiments

First, we tested the performance of the feedforward architecture in adapting to the visuomotor rotation. Analyzing the normalised mean-squared (nMSE) velocity error / retinal slip, we found no significant difference in the learning trace when adaptation to different magnitudes of rotation ($\psi = [15, 135]$) were compared. Fig. 5(a) plots the average nMSE over time for $\psi = 45°$ which is representative of all values of ψ. The error bars represent one standard deviation above and below the mean.

We then tested the performance of the feedforward architecture in adapting to novel dynamics. Fig. 5(a) plots the evolution of the nMSE over time for different values of ϕ. For $\phi = 15°$, performance is the same as under the visuomotor rotation. As ϕ increases, however, the rate of improvement drops. Error bars are plotted for the $\phi = 60°$ case to show that this difference is significant (error bars on other plots are omitted for clarity). At $\phi = 90°$, the VOR no longer converges and updates of the cerebellar weights no longer improve performance. This is equivalent to always moving perpendicularly to the direction of steepest slope. For $\phi > 90°$, changes in the cerebellar weights led to deteriorating performance and unstable adaptation.

For the recurrent architecture, we first tested the performance under the change in dynamics. For $\phi < 60°$, we found no significant difference in performance between different values of ϕ. For larger values of ϕ, however, the recurrent loop tended to become unstable after a period of initial improvement. Fig. 5(b) shows the nMSE over time for $\phi = 45°$ which was representative of all trials for $\phi < 60°$.

Finally, we tested the performance of the recurrent architecture in adapting to the visuomotor rotation. Results from these trials are also plotted in Fig. 5(b). Again, for clarity, error bars are only plotted for representative transformations. For $\psi = 15°$, performance is similar to that under the change in the dynamics. For $\psi = 45°$, however, the adaptation is significantly slower. For $\psi = 50°$ and greater, the recurrent loop tended to become unstable resulting in an exponential increase of the error over a very short timescale. The plots have therefore been curtailed at this point. The initial rate of improvement in performance is nevertheless reflective of the quality of the estimate of the cerebellar output error.

As predicted by the theory, performance of the feedforward architecture was impaired following changes in the oculomotor plant dynamics, but was not affected by changes in the kinematics. Performance of the recurrent architecture, on the other hand, was affected by changes in the kinematics but not by changes in the dynamics.

The inherent problem of instability in the brainstem-cerebellum loop under the recurrent architecture can be attributed, in a control theoretic way, to the eigenvalues λ of the matrix BC (refer Fig. 3(b)) having magnitude $|\lambda| > 1$. It may, however, be possible to avoid entering into unstable regions of the parameter space by adapting B, using C as a training signal. This 'learning transfer' from C to B would steer the loop away from regions of instability by ensuring that C^* (which would now depend on B) would tend asymptotically to 0. Learning transfer of this kind is supported by physiological evidence (Lisberger *et al.* 1994) and Dean and Porril (2004) have suggested it may be used as a mechanism to enhance VOR response at high frequencies.

4 Application to Saccade Adaptation

So far we have described adaptation of the VOR in response to two distinct kinds of sensorimotor transformations – changes in the motor command-outcome mapping and changes in the stimulus-desired outcome mapping. In this section, we show how the same arguments carry over to the saccadic system and in particular how different transformations affect the timecourse of learning under different cerebellar architectures.

Saccades are rapid eye movements used to change gaze fixation from one point to another. It is known that saccades are planned as a difference vector in retinotopic coordinates between the current fixation point and the desired fixation point (Hopp and Fuchs 2004). An open-loop sequence of motor commands based on this different

vector is then generated in the brainstem to guide the eye to the planned new position along a stereotyped trajectory (Hopp and Fuchs 2004).

The *gain* of a saccade is the ratio between the distance of the planned saccade and the distance the eye ultimately moves. Under ordinary circumstances the gain of the saccadic system should be equal to 1, but through physical changes to the eye or experimental intervention, systematic errors in the saccadic endpoint can be induced. Whenever such errors are experienced, the gain of the saccadic controller is adapted so as to reduce future errors. As in the VOR, this adaptation is believed to be cerebellar-dependent (Optican and Robinson 1980), motivating us to develop a pair of cerebellar-based models of saccade adaptation by analogy with the VOR adaptation models presented above. First we describe how the two different types of sensorimotor transformations are manifested in saccadic gain adaptation.

[Fig. 6 about here.]

4.1 Experimental saccade adaptation paradigms

Two different experimental paradigms have primarily been used to elicit adaptation of saccadic gain. One method is to surgically weaken one or more of the extraocular muscles by partially severing it. This procedure directly alters the plant dynamics so that the same motor command (stimulation of the extraocular muscles by motor neurons) will result in a different (smaller) eye movement, and therefore falling into the category of a change in the motor command-outcome mapping. Initially, the impaired eye will fall short of its target but, after practice, will adapt and eventually exhibit more accurate saccades.

The saccadic gains for each eye tend to adapt in tandem: if one eye is patched while the other undergoes gain adaptation, the gain of saccades in the patched eye will also change. Therefore, by weakening only one eye and by alternately patching either the good eye or the weakened eye, adaptation can be repeatedly induced either from low gain to normal gain (moving the patch from the weakened eye to the normal eye) or from high gain to normal gain (moving the patch from the normal eye to the weakened eye) (Scudder *et al.* 1998).

An alternative, non-surgical method to elicit adaptation of saccadic gain, first introduced by McLaughlin (1967), is to surreptitiously move the position of the target during the saccade (see Fig. 6). Subjects are unable to see this movement since vision is suppressed during saccades. If the target is shifted further away from its original position, this has a similar effect to having weakened muscles in that there is still some distance to go to the target at the end of the saccade. After many trials (typically thousands), the saccadic system adapts and the size of saccades changes to reduce the endpoint error.

Although it is tempting to view the latter experimental paradigm as a way of simulating a change in the plant dynamics, it should, in fact, be viewed as a change in the relationship between the stimulus and the desired outcome. The plant dynamics, that is the relationship between motor commands and ensuing eye movements, remain constant throughout. The shifted target location depends only on the original position of the target and not on the intermediate motor commands or the final eye position.

4.2 Implications for learning

Following the discussion of VOR adaptation in the previous section, we should likewise expect these different training paradigms to elicit different patterns of adaptation, depending on the organization of the underlying cerebellar-brainstem connectivity.

During the target shifting paradigm, targets are usually shifted parallel to the initially planned saccade and therefore the estimate of the cerebellar output under the recurrent architecture will then be inflated or shrunk, rather than rotated as in our VOR example. This will, however, affect the rate of adaptation as it effectively scales the learning rate β in (9). The same applies to learning under the feedforward model following changes in the dynamics. For the recurrent architecture, however, the rate of cerebellar learning does not necessarily reflect the rate of improvement in task-space due to non-linearities introduced in the recurrent loop. We will examine these effects in detail, specifically with respect to the time-course of learning.

4.3 Saccade adaptation model

In order to make concrete arguments about the role of the cerebellum and the impact of different training paradigms on the timecourse of learning, we introduce a simplified model of the saccadic system, illustrated in Fig. 7. In this section, for mathematical simplicity, we represent all variables as scalars and assume all mappings are linear. The stimulus, x, in this case is the initial target location relative to the current eye position. The brainstem B issues a sequence of motor commands based on this target location which we represent by a single scalar u characterizing its magnitude.

We model the plant dynamics as a simple linear relationship between motor command u and final eye position y, i.e.

$$y = P_0 u, \tag{33}$$

where P_0 denotes the normal plant dynamics. We model the surgical weakening of the eye by replacing P_0 with P_1 in (33) with $P_1 < P_0$. To model the target shift

paradigm, we assume that the mapping S is linear, corresponding to a change in the required gain, i.e.

$$y^* = S_1 x \tag{34}$$

so that S_1 is the new gain to be learned. The baseline (i.e. before adaptation is elicited) saccadic gain is assumed to be equal to 1. The distance remaining to the target $\widetilde{y} = y^* - y$ is the raw performance measure used to drive adaptation - analogous to the retinal slip in VOR adaptation. We consider a simplified experiment in which only unidirectional saccades are made with the distance x to the initial target kept constant.

[Fig. 7 about here.]

By analogy with the VOR, we assume the adaptive capabilities of saccades arise from a cerebellar pathway working in tandem with the brainstem B and that the cerebellar weights are updated on a trial-to-trial basis based on an estimate of the cerebellar output error.

We now seek to describe the time-course of learning mathematically under both the feedforward and recurrent architectures, and examine how the various parameters P_1,S_1 and x affect this time-course. Since saccade adaptation typically takes place over timescales of thousands of saccades, it seems reasonable to adopt a continuous-time approximation to simplify the derivations, rather than describing the trial-to-trial learning dynamics as a discrete-time dynamical system.

4.3.1 Feedforward Architecture

First, we note that the motor command u is generated as the sum of brainstem and cerebellar outputs,

$$u = Bx + Cx. \tag{35}$$

The observed error in the eye position is given by $\widetilde{y} = y^* - y$. Substituting the expressions for y and y^* into this we obtain

$$\widetilde{y} = S_1 x - P_1(Bx + Cx) \tag{36}$$

and taking the time derivative we have

$$\dot{\widetilde{y}} = -P_1 x \dot{C}, \tag{37}$$

where $\dot{C}$ corresponds to the rate of cerebellar weight adaptation as given by the cerebellar learning rule. We will assume the same gradient descent cerebellar learning rule as we employed for VOR adaptation (Section 2.1), i.e.

$$\dot{C} = \beta x P_0^{-1} \widetilde{y}. \tag{38}$$

Note that we use the old dynamics P_0 and the not the new dynamics P_1 to approximate the motor error, since the new dynamics are unknown. Substituting this into (37), we obtain

$$\dot{\widetilde{y}} = -\beta x^2 \frac{P_1}{P_0} \widetilde{y}. \tag{39}$$

This can easily be solved to reveal exponential decrease in performance error over time. Crucially this performance error is independent of S_1, i.e. the relationship between the initial target location (the stimulus) and the shifted target location (desired outcome).

4.3.2 Recurrent Architecture

For the recurrent architecture, as in the case of the VOR, the motor command u satisfies

$$u = B(x + Cu). \tag{40}$$

Rearranging and substituting this into the definition of $\widetilde{y}$ we have

$$\widetilde{y} = S_1 x - \frac{P_1 B x}{1 - BC}. \tag{41}$$

Taking the derivative with respect to time, we obtain

$$\dot{\widetilde{y}} = \frac{-P_1 B^2 x}{(1 - BC)^2} \dot{C}. \tag{42}$$

Again, $\dot{C}$ is given by the cerebellar learning rule. According to the theory presented in Section 2, the error in the cerebellar output is obtained by transforming the observed eye position error $\widetilde{y}$ via the inverse of the stimulus-desired outcome mapping. In this case, this yields $e_C = \widetilde{y}$ (since we assume initially $S = 1$, i.e. the target does not move) and the full cerebellar learning rule is then given by

$$\dot{C} = -\beta u \widetilde{y}. \tag{43}$$

Substituting this into the equation above, we have

$$\dot{\widetilde{y}} = -\beta P_1 x \left(\frac{B}{1 - BC} \right)^3 \widetilde{y}. \tag{44}$$

Finally, by rearranging (41) we can obtain an expression for $B/(1-BC)$ which we can substitute in here to obtain

$$\dot{\widetilde{y}} = -\beta P_1 x \left(\frac{S_1 x - \widetilde{y}}{P_1 x} \right)^3 \widetilde{y}. \tag{45}$$

[Table 1 about here.]

Table 1 summarizes the difference in learning dynamics between the two architectures. Note that these equations describe both the sensitivity to changes in the dynamics ($P_0 \rightarrow P_1$) and to shifting of the target ($S_1 \neq 1$).

The most significant different between the two architectures is in what parameters affect the timescale

of learning. The rate of learning in the feedforward architecture depends only on the initial plant dynamics P_0 (i.e. the dynamics model assumed to estimate the motor error), the novel plant dynamics P_1 and the initial distance to the target, x (regardless of whether or not it is subsequently shifted). It is independent of any change in gain (i.e. target-shifting) so that no difference in learning rate should be observed between large gain changes and small gain changes. In the recurrent architecture, on the other hand, the adaptation rate depends on the novel plant dynamics P_1 and the target shift size S_1, as well as the initial distance to the target x.

Another notable difference is that the feedforward architecture predicts an exponential decay of the learning rate over trials. The equation governing learning under the recurrent architecture, on the other hand, is nonlinear and does not predict purely exponential decay. This is ultimately due to the fact the learning rule (9) was devised to minimize the error in the cerebellar output and this has a nonlinear relationship with the performance error $\widetilde{y}$.

4.4 Simulation of saccade adaptation

[Fig. 8 about here.]

We simulated trial-to-trial adaptation and subsequent recovery of saccades under both the target shift and surgical weakening paradigms. In addition to the elements of the model described above, we introduced signal-dependent noise in the motor command so that the actual output of the plant on trial n was given by

$$y_n = P_1 u_n (1 + \epsilon_n), \tag{46}$$

with the ϵ_n's independent and drawn from a normal distribution, $\epsilon_n \sim N(0, .05^2)$. The value of .05 for the standard deviation of the distribution was chosen to give a spread of saccades and timecourse of learning which visually resembled the data presented in Straube *et al.* (1997). Similarly, a value of 2×10^{-5} was chosen for the learning rate β. The same value was used for both the forward and recurrent architectures. Further implementation details can be found in Appendix A.

Figure 8 shows the simulated data for adaptation and subsequent recovery to a gain decrease of 30% induced by target-shifting. The top pair of figures shows the data for adaptation under the feedforward architecture while the middle pair of figures shows the data for adaptation under the recurrent architecture. Experimental data from Straube *et al.* (1997) is shown below for comparison. Each dot represents the magnitude of an individual saccade while the solid line displays the results of adaptation in the noiseless case to more easily see the trend.

The clearest difference between the feedforward and recurrent architectures is observable in the recovery phase, where adaptation under the recurrent architecture exhibits an initially linear decrease in the error which tails off to an asymptote at around 1500 saccades. Under the feedforward architecture, on the other hand, a much sharper increase in performance is visible over the first few hundred saccades.

4.5 Comparison with experiment

Experimentally, the rate of saccade adaptation is typically estimated as the rate-constant (measured in number of saccades) of an exponential curve fitted to the data. In the context of our model, the trend of adaptation under the feedforward architecture truly is exponential, while for the recurrent architecture, an exponential still offers a reasonably good fit, despite the nonlinearities in the adaptation dynamics.

An experiment by Scudder *et al.* (1998) in fact directly compared the timecourse of learning across the two paradigms. The learning rates were estimated by fitting exponentials as described above. The authors found that, in adapting to overshoots, adaptation under the target-shift paradigm was markedly faster than under the surgical weakening paradigm. This pattern seems to be predicted by the feedforward architecture slightly more reliably than by the recurrent architecture. This pattern, however, was not repeated when adapting to undershoots.

Straube *et al.* (1997) examined how various properties of the timecourse of saccadic gain adaptation varied with the change in gain and with the change in the initial distance to the target while adapting under the target shifting paradigm. They found that changing the size of the planned saccade had little effect on the rate constant of the fitted exponential. Decreasing the gain, however did affect the rate of adaptation with more substantial gain decreases having a larger rate constant and therefore slower adaptation. This observation is certainly compatible with a recurrent architecture model. Under the feedforward architecture, our simplified model predicts that a change in gain should have no impact on the learning rate.

However, complicating the interpretation of these results is the fact that the effect of errors on learning (i.e. the cerebellar learning rule in our model) appears to depend strongly on the size of the error itself (Straube *et al.* 1997) and even the sign of the error (Robinson *et al.* 2003) (i.e. the learning rule is not linear in $\widetilde{y}$). Deviations from the idealized squared-error descent learning rule we assumed could potentially have a far greater impact on the timecourse of learning than the difference between architectures.

4.6 Other experimental paradigms

Not all saccade adaptation experiments follow the target-shifting paradigm we described here. Robinson *et al.* (2003) performed an experiment in which the position of the shifted target depended on the final eye position in such a way that the perceived error ($\widetilde{y}$) remained constant, irrespective of the actual final eye position. A study by Albano (1996) also varied the target location in response to the eye position. Unfortunately, neither of these studies present any data on the timescales of adaptation, which would potentially enlighten the present discussion.

The hardest aspect of adaptation to account for in these models is the potentially different adaptation response following different kinds of errors. We assumed that the learning rule acted to minimize the squared error $\widetilde{y}^2$. This 'cost function' may not, however, be appropriate. Several studies have commented that overshoot errors have a greater effect on adaptation than undershoot errors (Robinson *et al.* 2003; Hopp and Fuchs 2004).

Precise control over the errors experienced by subjects may enable a more detailed identification of the learning algorithms at the cerebellar level. Methods like this also offer the possibility of directly simulating a change in the plant dynamics by shifting the target in a way which is consistent with a weakened muscle.

In conclusion, we have shown how the two primary experimental paradigms for inducing saccadic gain adaptation are fundamentally different in nature - surgical weakening of the extraocular muscles manipulates the relationship between the motor command and the observed outcome, while the intra-saccadic shift paradigm manipulates the relationship between the stimulus and the desired outcome. We have outlined how, in principle, the empirical differences between the two architectures could be explained by a mathematical model of cerebellar-based error-driven learning. Currently available data, however, does not seem to be sufficient to infer both the learning rules and the underlying architecture of connectivity. Nevertheless, we have highlighted how the timecourse of learning can differ between the different learning architectures. Although we have illustrated these aspects of the alternative cerebellar-based learning models in the context of a relatively simple model, the basic insights in this section apply quite generally.

5 Reaching and Catching

Up to this point, we have only considered motor tasks which involve linear mappings between motor command and outcome and between stimulus and desired outcome. In Section 2, we claimed that our arguments concerning the required error signals for training the cerebellar pathway under different architectures and the ensuing properties of adaptation applied equally to nonlinear systems. In this section we demonstrate this explicitly by applying the two alternative architectures to the kinematic control of a two-link planar arm, along the lines of the model presented in Porrill and Dean (2007). We first, however, discuss the extent to which the cerebellar-based adaptation models presented in previous sections provide a good model of the role of the cerebellum in reaching, and then consider to what extent arm control is susceptible to changes in the motor command-outcome mapping and changes in the stimulus-desired outcome mapping.

While the exact role of the cerebellum in reaching movements is not entirely understood, cerebellar involvement has been demonstrated in compensating for interaction torques between limb segments (Bastian *et al.* 1996), adapting to altered dynamics (Smith and Shadmehr 2005) and visual feedback (Baizer *et al.* 1999) and in learning to manipulate an on-screen cursor (Imamizu *et al.* 2000). The role of motor command generation in reaching is largely attributed to the primary motor cortex (Todorov 2000; Shadmehr and Wise 2005). It therefore seems reasonable to extend the cerebellar-based adaptation frameworks for VOR and saccades from sections 2 and 4 to model the cerebellum's role in reaching adaptation. Indeed, Schweighofer *et al.* (1998) have suggested that the cerebellum generates feedforward motor commands which refine those generated by the cortex, implying the use of a feedforward cerebellar architecture.

By contrast, Porrill and Dean (2007) have proposed a model of arm control which employs a recurrent cerebellar architecture to learn an inverse kinematics model of the arm. In their model, the stimulus is a desired hand location, the motor command is a set of joint angles and the outcome is the actual hand position. Only the relationship between the joint angles and the resulting hand position is assumed to be subject to change. The stimulus and the desired outcome are always identical and this means the error in hand position equals the error in the cerebellar output. However, as in previous sections, if the relationship between the stimulus and desired outcome changes, then the hand position error will no longer reflect the error in the cerebellar output.

Conventional experimental paradigms for eliciting adaptation of reaching movements include application of an external force field to the hand via a robotic manipulandum (e.g., Shadmehr and Mussa-Ivaldi (1994)), or tampering with visual feedback - usually in the form of a rotation of the visual field about the initial position of the hand (Krakauer *et al.* 2000). Both of these manipulations amount to changing the relationship between the motor command and the eventual observed outcome.

Changes in the relationship between stimulus and desired outcome are not nearly as common in reaching as they are in oculomotor control. There are isolated examples of experiments that have elicited adaptation

to transformations of this kind. Lurito *et al.* (1991) performed an experiment in which Monkeys learned to make reaching movements in a direction 90^o rotated from the direction of an initial stimulus. Such sensorimotor mappings which involve a combination of stimulus-desired outcome and motor command-outcome mappings that must be learnt in the target-shifting experiment by Lurito *et al.* (1991) have been referred to as 'non-standard' or 'transformational' mappings (Shadmehr and Wise 2005), since the desired hand position is a transformed version of the initial stimulus location.

It is not too difficult to imagine circumstances in which the ability to learn mappings of this kind may be useful in arm control. For instance, when catching a ball, a catcher might learn to predict the trajectory of the ball from its state mid-flight and choose a suitable position along this trajectory at which to catch the ball. The movement of the hand to this intermediately calculated position can then be made using the existing reaching circuitry. It may, however, be beneficial to learn a direct relationship between the mid-flight state of the ball and the arm movements which will result in a succesful catch. Such a direct strategy would lead to lower latency and introduce less noise than having to maintain an intermediate representation of a desired hand location.

In the case of this catching example, any change in ball dynamics - e.g. on a windy day or with a ball more prone to air resistance, will affect the relationship between the mid-flight state of the ball (the 'stimulus') and the required hand position. Likewise, any distortion of visual feedback will affect the relationship between the stimulus and the desired hand position (unlike in the case of visually-guided point-to-point reaching movements), since the perceived trajectory of the ball will be different. Any change in arm kinematics or dynamics, for instance if trying to catch the ball using a net on the end of a heavy pole (note that this would affect both kinematics and dynamics!), will affect the relationship between motor command and resulting end-effector motion.

On these grounds we believe it is not unreasonable to consider a model of reaching in which the relationship between the stimulus and the desired outcome is subject to change. For simplicity we model this variability by target-shifting as in the experiment in (Lurito *et al.* 1991), but this can be thought of as an abstract version of the more involved 'catching' model outlined earlier.

5.1 Simulations

[Fig. 9 about here.]

Reaching Model

Reaching movements appear, like saccades, to be planned as a visually estimated difference vector $\mathbf{dx}$ between current hand location and target location in a retinotopic coordinate frame (Krakauer *et al.* 2000). A simplified model is illustrated in Fig. 9. Based on this difference vector, a suitable change in joint angles $\mathbf{du}$ is selected by the fixed controller B. We maintain our label B for this controller from the previous models of the VOR and saccades where it denotes 'brainstem', although here it denotes primary motor cortex. In general, the 'motor command' $\mathbf{du}$ will depend also on the current set of joint angles $\mathbf{u}$; for simplicity, in our experiments, we consider a unique starting joint position $\mathbf{u}$. The final observed hand position is then given by the kinematics P which represents a mapping from the change in joint angles $\mathbf{du}$ to a change in observed hand position $\mathbf{dy}$,

$$\mathbf{dy} = P(\mathbf{du}). \tag{47}$$

Note that this P includes both the forward kinematics of the arm, which map joint angles into hand position, and any distortions of visual feedback such as a rotation about the initial hand position.

Meanwhile, the target may be shifted mid-reach with the shift S determining the difference vector $\mathbf{dy}^*$ of the shifted target (and therefore, the desired observed change in hand position),

$$\mathbf{dy}^* = S(\mathbf{dx}). \tag{48}$$

The error $\widetilde{\mathbf{y}}$ in the observed hand position is used to guide adaptation of the controller and is given by the difference between the two,

$$\widetilde{\mathbf{y}} = \mathbf{dy}^* - \mathbf{dy}. \tag{49}$$

Adaptation in our model is mediated by the cerebellar pathway which may be connected with either a feedforward or recurrent architecture. The cerebellar output is constructed from a weighted sum of radial basis functions defined over the input space. The combination weights are learnt using the same gradient-descent learning rule as in previous sections, with the error in the cerebellar output estimated by transforming the error in hand position appropriately according to the architecture used, as described in Section 2. More technical details are given in Appendix A.

Experiment

[Fig. 10 about here.]

We set up a 10×10 square grid of targets around the initial position of the hand (given by the initial joint-angles $\boldsymbol{\theta}_0$ (see Fig. 10(a)). The goal was to find a suitable change of joint angles $\mathbf{du}$ such that the resulting change in hand position brought the hand in line with the target.

Two separate conditions were chosen requiring adaptation, the first corresponding to a change in the stimulus-desired outcome mapping, the second a change in the motor command-outcome mapping.

In the first condition, we implemented a target-shifting paradigm along the lines of the experiment presented in

(Lurito *et al.* 1991). During the reach, the position of each target was shifted by rotating it about the initial hand location by an angle $-\psi$.

In the second condition, we implemented a rotation of the visual field by angle ϕ about the initial hand location. This led to a rotation of the stimulus $\mathbf{dx}$ and also of the estimated error $\widetilde{\mathbf{y}}$ by the same amount. To ensure that the set of stimuli used (i.e. visually estimated difference vectors $\mathbf{dx}$) was the same in both conditions, the grid of targets was rotated by angle $-\phi$ during the visual field rotation. The mapping to be learnt by the cerebellum C and the set of stimuli used were the same in either condition provided $\phi = \psi$. The only difference between conditions, therefore, was in the nature of the error signal and how it related to the error in the cerebellar output.

A sequence of 200 reaching movements was simulated to a random sequence of the 100 targets and this was repeated 100 times with different randomly selected target sequences. The same target sequences were used for each architecture and for each condition. Figure 10 illustrates the results of learning under the different architectures and across the two different conditions. In particular, (d) and (e) show the normalized mean squared global test error (nMSE), averaged over all targets and all sessions, as a function of the number of reach trials performed for visual and target rotations of 45 °. For the feedforward architecture, it is particularly clear that performance is impaired under the visual rotation condition relative to the target rotation condition, in accordance with the theory. For the recurrent architecture, there was less difference in performance between conditions with marginally better asymptotic average performance under the visual rotation condition.

To demonstrate more clearly the effect that different kinds of transformation had on the quality of learning for different architectures, we examined the trend in reach errors during learning for a small subset of targets (marked with dots in the grid in Fig. 10(a)). We sampled the final hand position obtained during test trials to these targets after every 10 training trials. Because of the strong effect of the order of training targets on learning, we averaged these positions over 100 different training runs with different randomly selected target sequences to obtain an impression of the general trends of learning in each condition. The paths of these average positions as training proceeds are plotted in Fig. 11. The actual target locations are marked by a '×'. For the feedforward architecture, under the target-shift condition (Fig. 11(b)), the error estimate used for training is almost equal to the true error and, consequently, the improvement from trial-to-trial comes close to following a straight line in task space. Under the visual rotation condition (Fig. 11(a)), however, the effect of using a poorer estimate of the error is clearly seen in the fact that the trial-to-trial trend in reach errors does not follow a straight line but an indirect, curved one.

Under the recurrent architecture, there is still a clear difference between the two conditions. However in the visual rotation condition (Fig. 11(c)), where we expect the cerebellar output error estimate to be correct, the trial-to-trial trend in final hand position is not straight, as in the feedforward / target shift combination, but has slight curvature. This is due to the nonlinear relationship between the improvement in the cerebellar weights and improvements in task-space as discussed in the context of saccadic gain adaptation in Section 4.3. So although the improvement in cerebellar weight-space takes the shortest path, this does not necessarily correspond to shortest path improvement in task space in the same way as it does for the feedforward architecture. In the target shift condition (Fig. 11(d)), the trend, although different, doesn't appear to be much worse than in the visual rotation condition.

To highlight the fact that learning in the recurrent architecture really was 'better' for the visual rotation condition than for the target rotation conditions, we quantified the quality of the estimate of the cerebellar output error in each condition by computing the overlap between the estimated and true error, given by $\widehat{\widetilde{\mathbf{c}}}^T \widetilde{\mathbf{c}} \,/\, \widetilde{\mathbf{c}}^T \widetilde{\mathbf{c}}$. An overlap of 1 or close to 1 indicates a good approximation while an overlap of 0 indicates that the estimated error and the true error are perpendicular. Table 2 shows how this overlap varies with increasing ψ and ϕ. As expected, the estimated error was close to perfect in the case of the feedforward architecture / target shift combination and the recurrent architecture / visual rotation combination, independent of the magnitude of the transformation. For the other two conditions (feedforward with visual rotation and recurrent with target rotation), the quality of the estimate clearly diminished with increasing extent of visual field or target rotation.

As in the case of the VOR, the recurrent architecture was unstable in some circumstances with divergence of the motor command during iteration of the recurrent loop. For transformations with $\psi > 60°$ or $\phi > 60°$, this led to a total breakdown of learning for all targets (indicated by '—' in the table). For transformations of magnitude $\psi = 45°$ or $\phi = 45°$ the divergence of the motor command was only apparent for some targets and not for others. This caused a large discrepancy between the estimated cerebellar output and the error in hand position for these particular targets, leading to the large variation in overlap recorded in Table 2.

[Fig. 11 about here.]

[Table 2 about here.]

6 Conclusions

We have highlighted the fact that there are two distinct ways in which conditions of a motor task may change requiring adaptation of the motor response. Firstly, there

can be a change in the relationship between motor command and observed outcome and, secondly, there can be a change in the relationship between the initial stimulus and the desired outcome. We have shown examples of each of these two kinds of change in VOR adaptation, saccadic gain adaptation and adaptation in reaching movements, drawing a coherent and unified picture of the adaptation required. In particular, in the case of oculomotor control, many common experimental paradigms should be classified in the latter category rather than the former.

While this distinction has been noted previously (Jordan and Rumelhart (1992); Shadmehr and Wise (2005)), our main theoretical contribution here has been to show that the type of change has significant implications for the suitability of different cerebellar-based learning strategies. If a feedforward organization of the cerebellar pathway is employed, the observed performance error must be transformed via the inverse of the motor command-outcome mapping in order to accurately reflect the error in the cerebellar output. If a recurrent cerebellar architecture is employed, then the observed performance error must be transformed via the inverse of the stimulus-desired outcome mapping.

In each case, if an approximate inverse mapping is used to transform the performance error into cerebellar output error, the quality of the approximation will affect the learning rate and may even result in total failure to learn if the approximated error and the true cerebellar output error are not correlated.

Through simulations, we have demonstrated the impact of different forms of sensorimotor transformations on both learning rates and learning stability in the case of the VOR, saccadic adaptation and reaching.

7 Discussion

The present work has explored the properties of a number of adaptive control frameworks in the context of a variety of biologically-inspired learning problems. It is difficult, however, to draw any firm conclusions on what framework the brain uses in general, given the data currently available. It is possible that by systematically and independently transforming the stimulus-desired outcome and motor command-outcome mappings of a task, a careful examination of the impact on learning rates and/or learnability may offer clues to the organization of the nature of the underlying cerebellar circuitry. Of the motor behaviours discussed here, saccadic adaptation would appear to be the most promising setting for exploring such phenomena; however, it should be noted that the apparent differences in learning rates between overshoots and undershoots and other unknowns of the exact cerebellar learning rules may prove problematic in inferring the underlying organization from behavioural data alone.

There are other ways in which the problem of adapting to both kinds of sensorimotor transformations can be solved. In particular, in the case of changes in the stimulus-desired outcome relationship, one possibility which has been proposed in the case of reaching is a target-substitution strategy (Shadmehr and Wise 2005) whereby the initial stimulus is remapped to an intermediate representation which matches the true desired outcome and is then mapped to a motor command via the inverse dynamics. This is in contrast to learning a single direct mapping as we have described above. This strategy has analogs in VOR adaptation (pre-processing of the vestibular signal) and saccadic gain adaptation (re-scaling of the difference vector).

How the intermediate target-substitution mapping might be learnt, however, and particularly how changes in the stimulus-desired outcome mapping might be distinguised from changes in the motor-command outcome mapping is unclear since both can give rise to the same error.

In reality it is quite likely that a combination of target-substitution and direct mapping strategies, as well as feedforward and recurrent strategies are employed by the nervous system. Some behaviours are likely to be more susceptible to certain kinds of disturbances than others, rendering either a feedforward or recurrent architecture more appropriate.

Biomimetic robotics often employ cerebellar-based adaptive control strategies. Understanding the nature of the disturbances which are likely to be encountered should guide selection of which style of architecture may be more appropriate. Finally, we have shown elsewhere (Haith and Vijayakumar 2007) that in certain cases both architectures can be employed concurrently in a feedback-error learning framework to ensure robust adaptation to both kinds of change, combining the advantages of each individual architecture to maximum effect.

Acknowledgements This work was funded in part by the UK EPSRC/MRC through the Neuroinformatics Doctoral Training Centre, University of Edinburgh and by the EU FP6 Integrated Project SENSOPAC. We thank John Porrill and Paul Dean for helpful discussions.

A Implementation Details

[Table 3 about here.]

[Table 4 about here.]

The same pattern of training was used and very similar control and learning algorithms were employed for simulating each of the behaviours discussed here. Table 3 outlines the basic algorithm underlying all of the simulations.

In each case, an initial motor command-outcome mapping P_0 and an initial stimulus-desired outcome mapping S_0 were specified. The algorithm then simulated cerebellar-based adaptation to a new pair of mappings P_1 and S_1 (in practice

only one was varied at a time) using either a feedforward (FF) or recurrent (REC) architecture.

A sequence of stimuli $\mathbf{x}_{1:T}$ was selected. For the VOR, this $\mathbf{x}_t$ represented a discrete-time series of head velocity measurements with a discretization timestep of $.01s$. For saccades and reaching, each $\mathbf{x}_t$ represented a difference vector movement plan for a single trial for the eye or hand, respectively.

The fixed controller B generates motor commands which are optimal under the initial conditions P_0 and S_0, i.e.

$$B(\mathbf{x}_t) = P_0^{-1}(S_0(\mathbf{x}_t)). \tag{50}$$

The input to the cerebellum, which we denote by $\mathbf{z}_t$, varied depending on the architecture employed and the task. For linear P and S (i.e. in the case of VOR and saccades), under the forward architecture this was equal to the stimulus $\mathbf{x}_t$, while under the recurrent architecture this was equal to the motor command $\mathbf{u}_t$.

For nonlinear P and S (i.e. reaching), $\mathbf{z}_t$ was given by a set of non-linear basis functions $\boldsymbol{\Phi}$ defined over the same input space, i.e. $\mathbf{z}_t = \boldsymbol{\Phi}(\mathbf{x}_t)$ for the feedforward architecture and $\mathbf{z} = \boldsymbol{\Phi}(\mathbf{u}_t)$ for the recurrent architecture. The basis functions $\boldsymbol{\Phi}$ were Gaussians given by

$$\Phi_i(\mathbf{o}) = e^{(\mathbf{o}-\mathbf{r}_i)^T \Sigma (\mathbf{o}-\mathbf{r}_i)}, \tag{51}$$

where $\mathbf{o}$ represents the appropriate input ($\mathbf{x}_t$ or $\mathbf{u}_t$) depending on the architecture. The function centres $\mathbf{r}_i$ were distributed on a uniform square grid in the input space and the metric Σ was chosen so that the width of each tuning function along each dimension was equal to twice the separation $\Delta\mathbf{r}$ between functions:

$$\Sigma = 2 \begin{pmatrix} \frac{1}{\Delta \mathbf{r}_1} & 0 & 0 \\ 0 & \ddots & 0 \\ 0 & 0 & \frac{1}{\Delta \mathbf{r}_n} \end{pmatrix}. \tag{52}$$

Note that $\mathbf{r}$ and Σ were different between the two architectures due to different distributions of inputs. A total of 16 basis functions in a 4×4 grid was used in each case.

The cerebellar output $\mathbf{c}_t$ was then given by mutliplying the input $\mathbf{z}_t$ by the learnt cerebellar weight matrix W_t,

$$\mathbf{c}_t = W_t \mathbf{z}_t. \tag{53}$$

The motor command $\mathbf{u}$ was constructed differently for different architectures. For the feedforward architecture, it was given directly by the sum of the cerebellar and brainstem outputs

$$\mathbf{u}_t = B(\mathbf{x}_t) + C(\mathbf{x}_t). \tag{54}$$

For the recurrent architecture, when approximating continuous time dynamics, as in the VOR, the motor command was calculated as

$$\mathbf{u}_t = B(\mathbf{x}_t + C(\mathbf{u}_{t-1})). \tag{55}$$

For simulating single trials of saccades and reaching, the motor command was determined by iterating the equation

$$\mathbf{u}_t = B(\mathbf{x}_t + C(\mathbf{u}_t)) \tag{56}$$

until the difference in $\mathbf{u}$ between successive iterations was less than 0.1 %.

In some cases the recurrency led to divergence of $\mathbf{u}_t$ either while iterating within a single trial (saccades and reaching) or over time (VOR), in which case the recurrent architecture was unstable and unable to learn the task. However, this was typically only an issue for transformations of moderate to large magnitude and for less severe transformations $\mathbf{u}_t$ converged within 10-20 iterations.

The motor command $\mathbf{u}_t$ was then transformed into an observed output $\mathbf{y}$ via the (transformed) plant dynamics P_1,

$$\mathbf{y}_t = P_1(\mathbf{u}_t). \tag{57}$$

For saccades and reaching the converged value of $\mathbf{u}_t$ was used for this. Additionally, for saccades, signal-dependent Gaussian noise was added to the motor command to give a realistic variation in saccadic amplitude:

$$\mathbf{y}_t = P_1(\mathbf{u}_t(1+\boldsymbol{\epsilon}_t));\ \boldsymbol{\epsilon}_t \sim N(0, 0.5^2) \tag{58}$$

The desired outcome at each timestep or trial, $\mathbf{y}_t*$, was calculated separately according to the (transformed) stimulus-desired outcome relationship,

$$\mathbf{y}_t^* = S_1(\mathbf{x}_t). \tag{59}$$

The observation error was then calculated as

$$\widetilde{\mathbf{y}}_t = \mathbf{y}_t^* - \mathbf{y}_t. \tag{60}$$

To estimate the error in the cerebellar output, the initial mappings between motor command and observed outcome P_0 and between stimulus and desired outcome S_0 were used, according to the theory presented in section 2, i.e. for the recurrent architecture,

$$\widehat{\widetilde{\mathbf{c}}}_t = \widetilde{\mathbf{y}}_t, \tag{61}$$

and for the feedforward architecture,

$$\widehat{\widetilde{\mathbf{c}}}_t = P_0^{-1}\widetilde{\mathbf{y}}_t. \tag{62}$$

Where this mapping was nonlinear (i.e. for reaching) the error was approximated to first order using a Taylor expansion,

$$\widehat{\widetilde{\mathbf{c}}}_t = J_{P_0^{-1}}(\mathbf{y}_t)\widetilde{\mathbf{y}}_t \tag{63}$$

where $J_{P_0^{-1}}(\mathbf{y}_t)$ is the Jacobian of P_0^{-1} at $\mathbf{y}_t$. This was estimated numerically by finite differences. Note that in all simulations S was linear, although the same principle could be used for approximating $\widehat{\widetilde{\mathbf{c}}}$ in the recurrent architecture if it weren't.

Finally, the cerebellar weights were updated at each time step using a discrete-time analog of the gradient learning rule stated in section 2.1

$$W_t = W_{t-1} + \beta \widetilde{\mathbf{c}}_t \mathbf{p}_t^T, \tag{64}$$

where $\widetilde{\mathbf{c}}_t$ is the *estimated* cerebellar output error.

The learning rate β was different in each case and chosen to give approximately realistic timescales of adaptation in comparison to experimental data. The same value of β was always used for both architectures.

References

Albano, J. E. (1996). Adaptive changes in saccade amplitude: oculocentric or orbitocentric mapping? *Vision Res*, **36**(14), 2087–2098.

Baizer, J., Kralj-Hans, I., and Glickstein, M. (1999). Cerebellar lesions and prism adaptation in macaque monkeys. *Journal of Neurophysiology*, **81**(4), 1960–1965.

Bastian, A., Martin, T., Keating, J., and Thach, W. T. (1996). Cerebellar ataxia: abnormal control of interaction torques across multiple joints. *Journal of Neurophysiology*, **76**, 492–509.

Coenen, O. J. and Sejnowski, T. J. (1996). A dynamical model of context dependencies for the vestibulo-ocular reflex. In *Advances in Neural Information Processing Systems*, volume 8, Cambridge, MA. MIT Press.

Dean, P. and Porril, J. (2004). Plant compensation in vestibulo-ocular reflex: Computational analysis points to multiple points of plasticity. Poster, Society for Neuroscience meeting.

Gomi, H. and Kawato, M. (1990). Learning control for a closed loop system using feedback-error-learning. In *Proceedings of the 29th conference on decision and control*, pages 3289–3294.

Haith, A. and Vijayakumar, S. (2007). Robustness of VOR and OKR adaptation under kinematics and dynamics transformations. In *Proc. Sixth IEEE international Conference on Development and Learning (ICDL '07), London, (2007).*

Hirata, Y. and Highstein, S. M. (2001). Acute adaptation of the vestibuloocular reflex: signal processing by floccular and ventral parafloccular Purkinje cells. *J Neurophysiol*, **85**(5), 2267–2288.

Hopp, J. J. and Fuchs, A. F. (2004). The characteristics and neuronal substrate of saccadic eye movement plasticity. *Prog Neurobiol*, **72**(1), 27–53.

Imamizu, H., Miyauchi, S., Tamada, T., Sasaki, Y., Takino, R., Putz, B., Yoshioka, T., and M., K. (2000). Human cerebellar activity reflecting an acquired internal model of a new tool. *Nature*, **403**(6766), 192–195.

Ito, M. (2000). Mechanisms of motor learning in the cerebellum. *Brain Research*, **886**(1-2), 237–245.

Jordan, M. I. and Rumelhart, D. E. (1992). Forward models: Supervised learning with a distal teacher. *Cognitive Science*, **16**, 307–354.

Kawato, M. and Gomi, H. (1992). The cerebellum and VOR/OKR learning models. *Trends in Neuroscience*, **15**(11), 445–453.

Krakauer, J. W., Pine, Z. M., Ghilardi, M. F., and Ghez, C. (2000). Learning of visuomotor transformations for vectorial planning of reaching trajectories. *J Neurosci*, **20**(23), 8916–8924. Clinical Trial.

Lisberger, S. G., Pavelko, T. A., Bronte-Stewart, H., and Stone, L. (1994). Neural basis for motor learning in the vestibuloocular reflex of primates. *Journal of Neurophysiology*, **72**(2), 954–973.

Lurito, J. T., Georgakopoulos, T., and Georgopoulos, A. P. (1991). Cognitive spatial-motor processes. 7. The making of movements at an angle from a stimulus direction: studies of motor cortical activity at the single cell and population levels. *Exp Brain Res*, **87**(3), 562–580.

McLaughlin, S. (1967). Parametric adjustment in saccadic eye movement. *Percept. Psychophys.*, **2**, 359–362.

Optican, L. M. and Robinson, D. A. (1980). Cerebellar-dependent adaptive control of primate saccadic system. *J Neurophysiol*, **44**(6), 1058–1076.

Porrill, J. and Dean, P. (2007). Recurrent cerebellar loops simplify adaptive control of redundant and nonlinear motor systems. *Neural Comput*, **19**(1), 170–193.

Porrill, J., Dean, P., and Stone, J. V. (2004). Recurrent cerebellar architecture solves the motor-error problem. *Proceedings in Biological Sciences*, **271**(1541), 789–796.

Robinson, F. R., Noto, C. T., and Bevans, S. E. (2003). Effect of visual error size on saccade adaptation in monkey. *J Neurophysiol*, **90**(2), 1235–1244.

Schweighofer, N., Arbib, M. A., and Kawato, M. (1998). Role of the cerebellum in reaching movements in humans. I. Distributed inverse dynamics control. *Eur J Neurosci*, **10**(1), 86–94.

Scudder, C. A., Batourina, E. Y., and Tunder, G. S. (1998). Comparison of two methods of producing adaptation of saccade size and implications for the site of plasticity. *J Neurophysiol*, **79**(2), 704–715. Comparative Study.

Shadmehr, R. and Mussa-Ivaldi, F. A. (1994). Adaptive representation of dynamics during learning of a motor task. *J Neurosci*, **14**(5 Pt 2), 3208–3224.

Shadmehr, R. and Wise, S. P. (2005). *The Computational Neurobiology of Reaching and Pointing: A Foundation for Motor Learning*. MIT Press.

Shibata, T. and Schaal, S. (2001). Biomimetic gaze stabilization based on feedback-error-learning with nonparametric regression networks. *Neural Networks*, **14**(2), 201–216.

Smith, M. and Shadmehr, R. (2005). Intact ability to learn internal models of arm dynamics in huntington's but not cerebellar degeneration. *Journal of Neurophysiology*, **93**, 2809–2821.

Straube, A., Fuchs, A. F., Usher, S., and Robinson, F. R. (1997). Characteristics of saccadic gain adaptation in rhesus macaques. *J Neurophysiol*, **77**(2), 874–895.

Todorov, E. (2000). Direct cortical control of muscle activation in voluntary arm movements: a model. *Nat Neurosci*, **3**(4), 391–398.

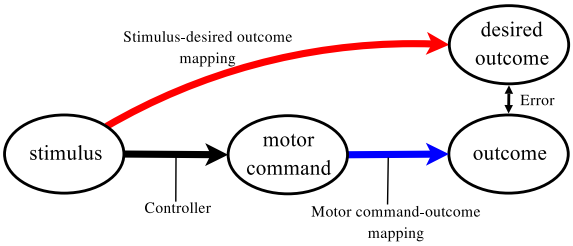

Fig. 1 Illustration of the two kinds of mappings described in section 1

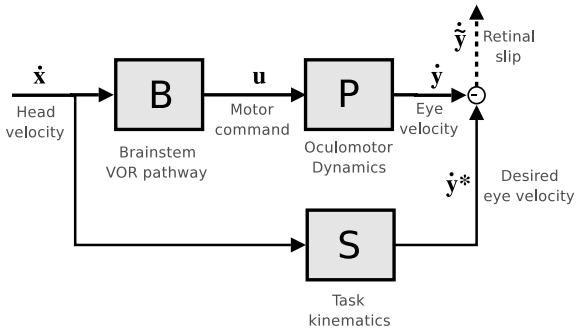

Fig. 2 Schematic of the VOR

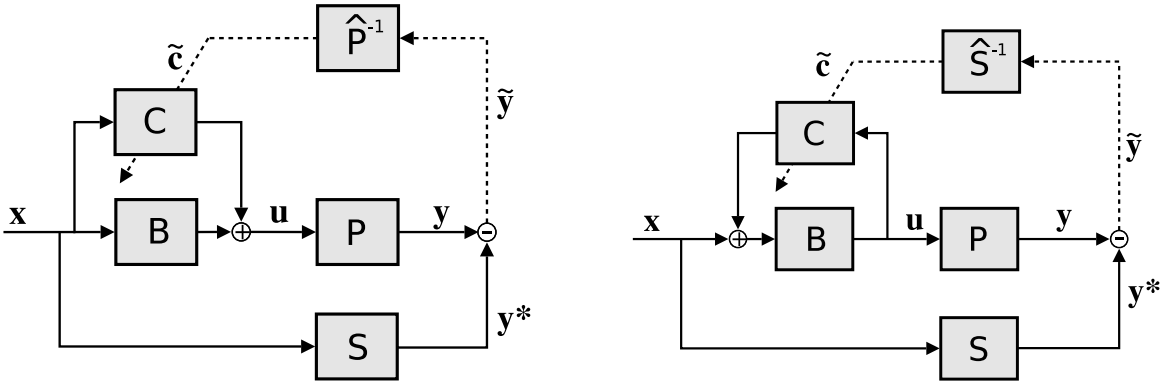

(a) Feedforward Architecture

(b) Recurrent Architecture

Fig. 3 Schematic of feedforward and recurrent architectures

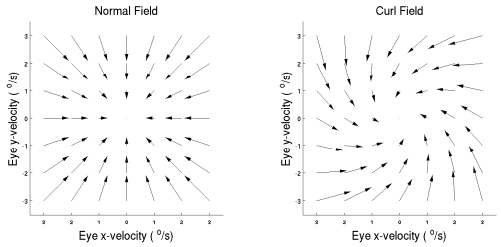

(a) Dynamics transformation

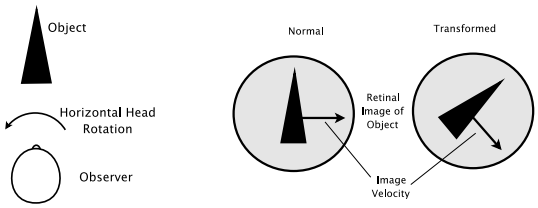

(b) Kinematics transformation

Fig. 4 Example of dynamic and kinematic transformations.

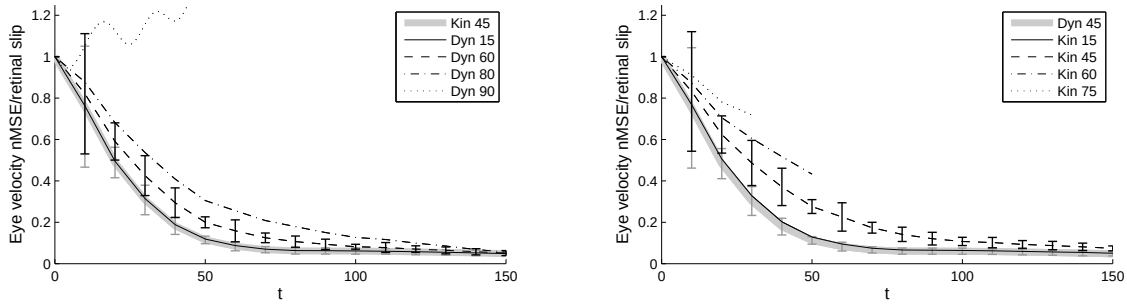

(a) Feedforward Architecture (b) Recurrent Architecture

Fig. 5 Timecourse of adaptation for VOR model using 5(a) feedforward architecture and 5(b) recurrent architecture. Both figures display average normalized mean squared eye velocity error (retinal slip), averaged over 10 trials. Different traces show response to different conditions - either a change in dynamics (viscous curl field) or a change in kinematics (visual field rotation) of differing magnitudes.

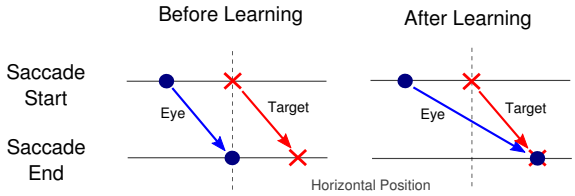

Fig. 6 Illustration of target shifting paradigm

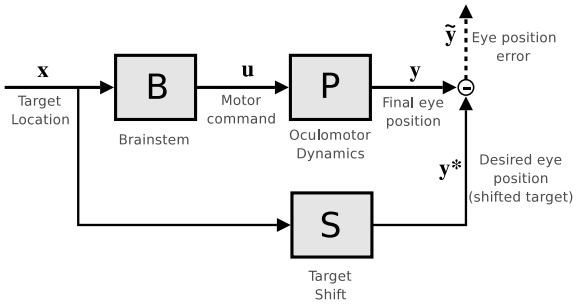

Fig. 7 Simplified saccadic adaptation framework

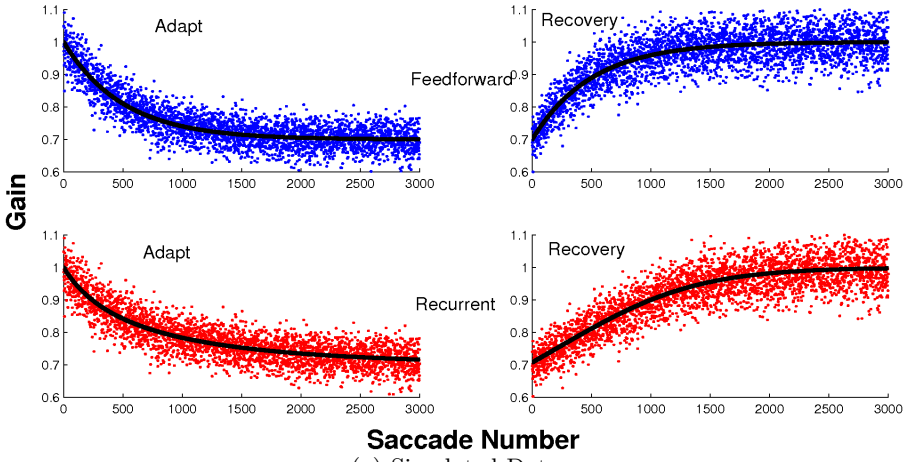

(a) Simulated Data

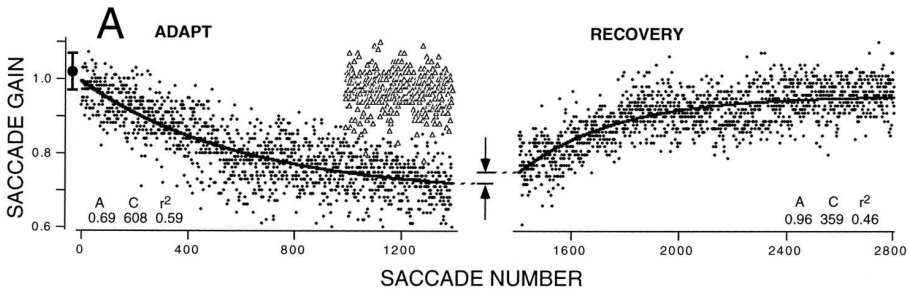

(b) Experimental Data

Fig. 8 Comparison of simulated saccadic gain adaptation and experimental data for the McLaughlin target-shifting paradigm. Simulated saccade adaptation trials under the feedforward architecture (top) and recurrent architecture (middle). Each scatter dot indicates gain of saccade for an individual trial. Solid black line indicates timecourse of learning in the noiseless condition. Experimental data are shown at the bottom, reproduced from (Straube *et al.* 1997) with permission.

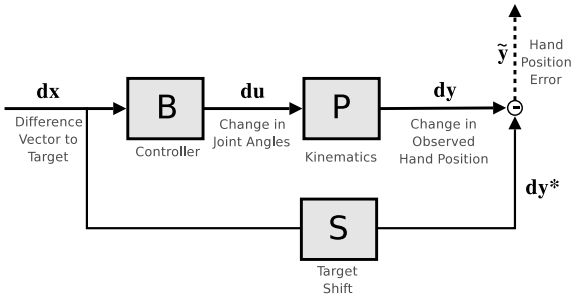

Fig. 9 Schematic of human reaching model.

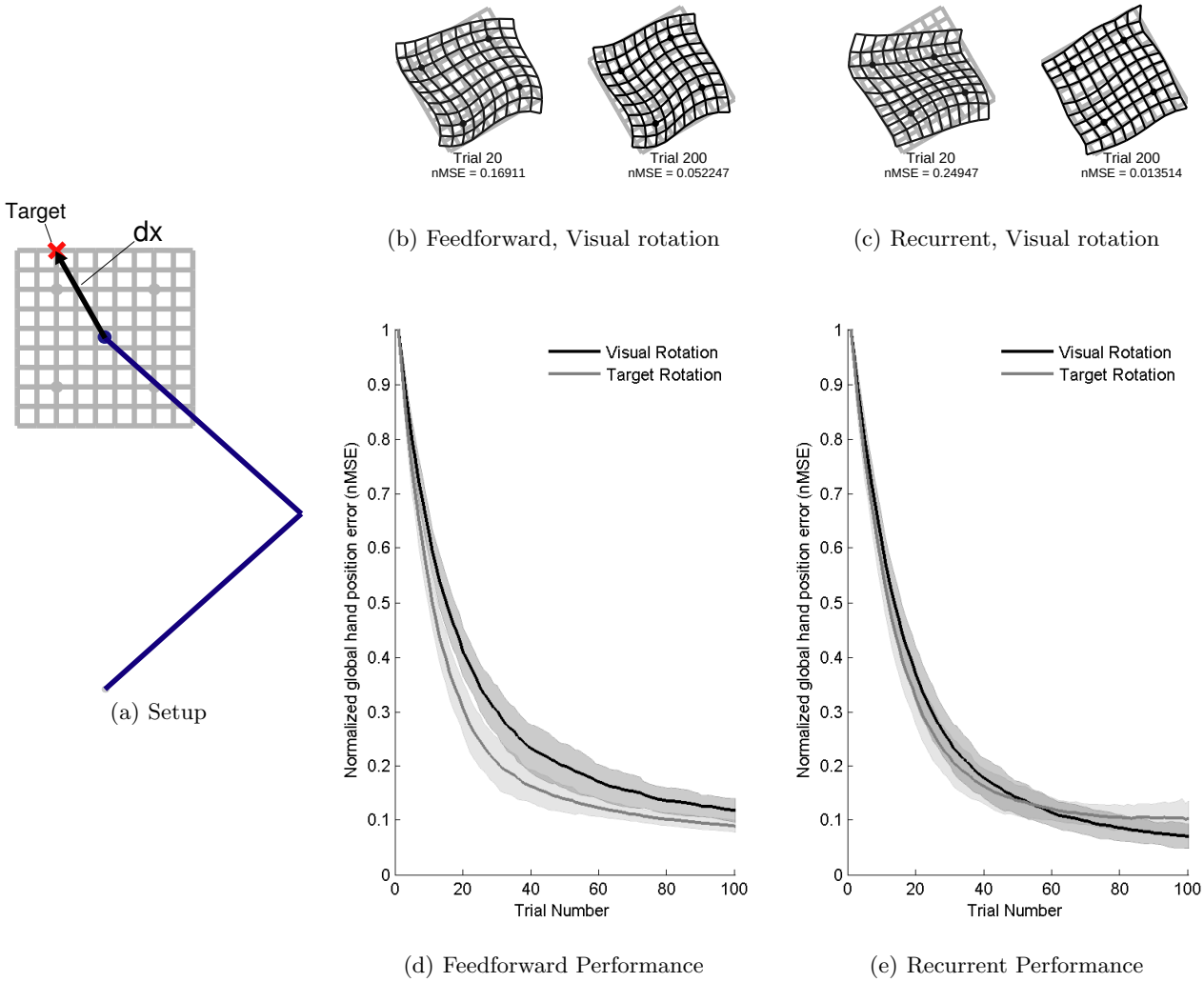

(a) Setup

(b) Feedforward, Visual rotation

(c) Recurrent, Visual rotation

(d) Feedforward Performance

(e) Recurrent Performance

Fig. 10 Learning kinematic control of a two-link planar arm. (a) Experimental setup of arm and grid of observed targets. Difference vector **dv** is estimated from seen target positions (which may be rotated from the actual positions) and this constitues the stimulus. (b)-(c) Grid of learnt hand positions following 30^o visual rotation for feedforward and recurrent architectures after 20 and 200 trials. Light grey grid shows the actual (rather than seen) final location of targets. Dark grid shows the grid of hand positions attained while testing reaching to all targets following the indicated number of training trials. (d) - (e) Normalized global mean squared hand position error as a function of the number of trials. Visual rotation and target rotation are compared for each architecture.

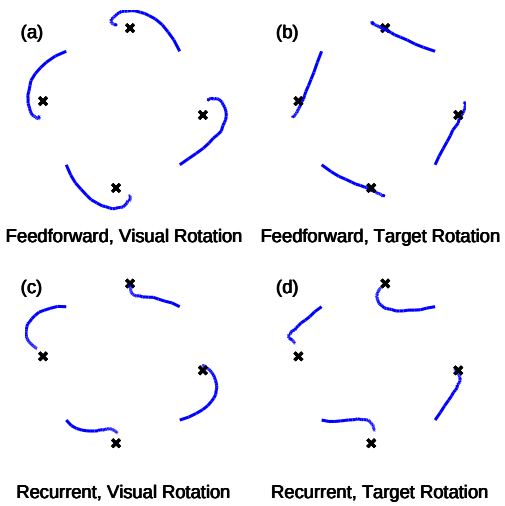

Fig. 11 Time-course of learning for selected targets

Table 1 Dynamics of learning for different adaptation strategies

Model	Error Dynamics
Feedforward	$\dot{\widetilde{y}} = \quad -\beta x^2 \frac{P_1}{P_0} \widetilde{y}$
Recurrent	$\dot{\widetilde{y}} = \quad -\beta P_1 x \left(\frac{S_1 x - \widetilde{y}}{P_1 x} \right)^3 \widetilde{y}$

Table 2 Quality of cerebellar output error estimates under different conditions.

		Average $\widehat{\mathbf{c}}^T\widetilde{\mathbf{c}} / \widetilde{\mathbf{c}}^T\widetilde{\mathbf{c}}$ ± (s.d.)					
Architecture	Condition	15 °	30°	45 °	60°	75 °	90°
Feedforward	Vis. Rotation	.96 ± .17	.87 ± .33	.72 ± .48	.49 ± .61	-.03 ± .15	-.04 ± .17
	Target Shift	1.00 ± .01	1.00 ± .01	1.00 ± .02	1.00 ± .02	1.00 ± .03	1.00 ± .03
Recurrent	Vis. Rotation	1.00 ± .00	.99 ± .11	1.05 ± 1.83	—	—	—
	Target Shift	.97 ± .00	.85 ± .11	.82 ± 2.24	—	—	—

Table 3 Pseudocode summary of algorithm used for all simulating all behaviours simulated and for both architectures. (Exceptions for particular behaviours are given in parentheses).

Initialize:
Define stimulus sequence $\mathbf{x}_{1:T}$
$W_1 = 0$
($\mathbf{u}_0 = 0$ for VOR)

Run:
For t = 1:T

1. **Generate motor command $\mathbf{u}_t$**
   if (FF)
   $\mathbf{z}_t = \mathbf{x}_t$ (or $\mathbf{z}_t = \Phi(\mathbf{x}_t)$ for reaching)
   $\mathbf{c}_t = W_t \mathbf{z}_t$

   if (REC)
   $\mathbf{u}_t = 0$
   iterate
   $\mathbf{z}_t = \mathbf{u}_t$ (or $\mathbf{z}_t = \Phi(\mathbf{u}_t)$ for reaching)
   $\mathbf{c}_t = W_t \mathbf{z}_t$
   $\mathbf{u}_t = B(\mathbf{x}_t + \mathbf{c}_t)$
   until convergence of $\mathbf{u}_t$:

   (or $\mathbf{u}_t = B(\mathbf{x}_t + \mathbf{c}_{t-1})$ for VOR)

2. **Calculate outcome $\mathbf{y}_t$ and observed error $\widetilde{\mathbf{y}}_t$**
   $\mathbf{y}_t = P_1(\mathbf{u}_t)$ ($\mathbf{y}_t = P_1(\mathbf{u}_t(1 + \boldsymbol{\epsilon}_t))$ for saccades)
   $\mathbf{y}_t^* = S_1(\mathbf{u}_t)$

   $\widetilde{\mathbf{y}}_t = \mathbf{y}_t^* - \mathbf{y}_t$

3. **Estimate cerebellar error $\widetilde{\mathbf{c}}_t$**
   if (FF)
   $\widehat{\widetilde{\mathbf{c}}}_t = P_0^{-1}(\widetilde{\mathbf{y}}_t)$ (or $\widehat{\widetilde{\mathbf{c}}}_t = J_{P_0^{-1}} \widetilde{\mathbf{y}}_t$ for reaching)

   if (REC)
   $\widehat{\widetilde{\mathbf{c}}}_t = S_0^{-1}(\widetilde{\mathbf{y}}_t)$

4. **Update cerebellar weights**
   $W_{t+1} = W_t + \beta \widehat{\widetilde{\mathbf{c}}}_t \mathbf{z}_t^T$

End

Table 4 Summary of model details for different behaviours.

Model Component	Notation	Description		
		VOR	Saccades	Reaching
Stimulus	$\mathbf{x}_t$	Head velocity	Target difference vector	Target difference vector
Outcome	$\mathbf{y}_t$	Eye velocity	Eye displacement	Hand displacement
Motor command	$\mathbf{u}_t$	Oculomotor torque	Motor amplitude	Change in joint angle
Motor command-outcome mapping	P	Oculomotor Dynamics	Oculomotor dynamics	Visual rotation
Stimulus-desired outcome mapping	S	Visual rotation	Target shift	Target shift